

*The influence of eddy parameterizations
on the transport of the Antarctic
Circumpolar Current in coupled climate
models*

Article

Accepted Version

Kuhlbrodt, T., Smith, R. S., Wang, Z. and Gregory, J. M. (2012)
The influence of eddy parameterizations on the transport of
the Antarctic Circumpolar Current in coupled climate models.
Ocean Modelling, 52-53. pp. 1-8. ISSN 1463-5003 doi:
<https://doi.org/10.1016/j.ocemod.2012.04.006> Available at
<https://centaur.reading.ac.uk/28371/>

It is advisable to refer to the publisher's version if you intend to cite from the
work. See [Guidance on citing](#).

To link to this article DOI: <http://dx.doi.org/10.1016/j.ocemod.2012.04.006>

Publisher: Elsevier

All outputs in CentAUR are protected by Intellectual Property Rights law,
including copyright law. Copyright and IPR is retained by the creators or other
copyright holders. Terms and conditions for use of this material are defined in
the [End User Agreement](#).

www.reading.ac.uk/centaur

CentAUR

Central Archive at the University of Reading

Reading's research outputs online

ABSTRACT

The transport of the Antarctic Circumpolar Current (ACC) varies strongly across the coupled GCMs (general circulation models) used for the IPCC AR4. This note shows that a large fraction of this across-model variance can be explained by relating it to the parameterization of eddy-induced transports. In the majority of models this parameterization is based on the study by Gent and McWilliams (1990). The main parameter is the quasi-Stokes diffusivity κ . The ACC transport and the meridional density gradient both correlate strongly with κ across those models where κ is a prescribed constant. In contrast, there is no correlation with the isopycnal diffusivity κ_{iso} across the models. The sensitivity of the ACC transport to κ is larger than to the zonal wind stress maximum. Experiments with the fast GCM FAMOUS show that changing κ directly affects the ACC transport by changing the density structure throughout the water column. Our results suggest that this limits the role of the wind stress magnitude in setting the ACC transport in FAMOUS. The sensitivities of the ACC and the meridional density gradient are very similar across the AR4 GCMs (for those models where κ is a prescribed constant) and among the FAMOUS experiments. The strong sensitivity of the ACC transport to κ needs careful assessment in climate models.

The influence of eddy parameterizations on the transport of the Antarctic Circumpolar Current in coupled climate models

T. Kuhlbrodt^a, R. S. Smith^a, Z. Wang^b, J. M. Gregory^{a,c}

^a*NCAS-Climate, Department of Meteorology, University of Reading, UK*

Email: t.kuhlbrodt@reading.ac.uk, phone: +44 (0)118 378 6014, fax: +44 (0)118 378 8316

^b*British Antarctic Survey, Cambridge, UK*

^c*Met Office, Exeter, UK*

Keywords: Antarctic Circumpolar Current, IPCC AR4 GCMs, Southern Ocean, Eddy parameterizations, Eddy-induced transports, Isopycnal diffusivity

1. Introduction

The Antarctic Circumpolar Current (ACC) is the strongest current in the world ocean. Its volume transport, measured in the Drake Passage, amounts to 137 ± 9 Sv (Cunningham et al. 2003). Its presence has a strong influence on the climate in Antarctica, and the meridional overturning circulation across the ACC transports substantial amounts of heat, carbon and other tracers (Shaffrey et al. 2009; Woloszyn et al. 2011).

In the coupled general circulation models (GCMs) used for the Fourth Assessment Report (AR4) of the Intergovernmental Panel on Climate Change (IPCC 2007), the ACC transport varies over almost one order of magnitude, between 37 Sv and 337 Sv (Fig. 1a). Russell et al. (2006) identified, in a qualitative way, the relevance of the resolved fields (like wind stress or salinity and temperature gradients) to this large spread, but a quantitative explanation has not been fully established yet.

The GCMs used for the AR4 come with ocean components that have a typical horizontal

39 resolution of one to two degrees. Therefore the mesoscale eddies are not resolved and their
40 effects on the large-scale circulation need to be parameterized. Almost all IPCC AR4 GCMs
41 use parameterizations that go back to (Gent and McWilliams 1990, hereafter cited as GM90).
42 One objective of the present note is to show the strong influence of this parameterization
43 (often dubbed simply “GM”) on the oceanic density field and the ACC transport across the
44 AR4 coupled climate models.

45 It is known that the GM parameterization generally improves the circulation in ocean
46 models (Danabasoglu and McWilliams (1995) and others; see Griffies et al. (2000) and
47 references therein). On a global scale, its effect is strongest in the Southern Ocean due
48 to the widespread outcropping of isopycnal layers. The density structure is improved, and
49 excessive open-ocean convection is significantly reduced. The sensitivity of the ACC to the
50 GM parameterization has been studied before in individual models (e.g. Danabasoglu and
51 McWilliams 1995; Gent et al. 2001) in an ocean-only setting. Our results show that the
52 across-model sensitivity within a subset of the AR4 coupled climate models is very similar
53 to the sensitivity of individual models.

54 We further explored the influence of GM on the ACC transport by conducting a sensitivity
55 study with a fast atmosphere-ocean GCM (AOGCM). This is an advantage over the earlier
56 sensitivity studies regarding κ that used an ocean-only setting with prescribed surface forcing,
57 precluding a reaction of the surface fluxes on the density changes in the ocean. In addition,
58 the fast AOGCM allows for runs that are long enough to let the ACC fully adjust—something
59 that could not be done in other recent studies of the GM parameterization using a coupled
60 GCM (e.g. Farneti and Gent 2011).

61 The isopycnal diffusivity κ_{iso} influences circulation and density structure, too (e.g. Sijp

et al. 2006), and equals κ in many models. We therefore tested the sensitivity of the ACC against κ_{iso} across the AR4 models as well as in FAMOUS.

The parameterized eddy-induced transports typically add up to a deep overturning cell across the ACC. However, for the AR4 climate models this overturning could not be diagnosed as the eddy-induced transports were not among the list of suggested variables for the CMIP3 exercise, and thus are not available. It was however possible to collect the information about the implementation of the GM parameterization in the individual models from various sources. We use the data of the 25 GCMs that participated in the Coupled Model Intercomparison Project Phase 3 (CMIP3) that was part of the IPCC AR4. The data are available at the Program for Climate Model Diagnosis and Intercomparison (PCMDI, http://www-pcmdi.llnl.gov/ipcc/about_ipcc.php). We have not considered the data that are currently being produced for the upcoming IPCC AR5 because at the time of writing data relevant for this study were available for only a small number of GCMs.

There are processes that the eddy parameterizations used by the AR4 climate models do not capture. One example is eddy saturation (Hallberg and Gnanadesikan 2006; Farneti et al. 2010). We do not address these processes here. Instead, our aim is to point out that the GM parametrization plays a strong role in setting the ACC transport and can dominate the wind stress as a driving force. This holds not only for individual models, but also across various AR4 climate models. We consider it likely that this will be true for the AR5 models too.

2. Parameterizing eddy-induced transports in GCMs

a. Parameterizations

Using an isopycnal framework, GM90 showed that, in a statistically steady state, the divergence of the flux of the mean density field by the mean velocity is approximately balanced by the divergence of a mean density flux due to mesoscale eddies. As a parameterization of this effect in non-eddy-resolving models they suggested a diffusion of isopycnal thickness $h = -\partial z / \partial \rho$, with the potential density ρ referenced to local pressure.

Gent et al. (1995) (hereafter cited as GWMM95) suggested formulating the thickness diffusion, in depth level coordinates, as an eddy-induced velocity that is added to the tracer advection equations:

$$\mathbf{u}^* = -\frac{\partial}{\partial z} (\kappa \mathbf{S}) ; w^* = \nabla_h \cdot (\kappa \mathbf{S}) , \quad (1)$$

where \mathbf{u}^* and w^* are the horizontal and vertical eddy-induced velocities, κ the eddy-induced thickness diffusivity and \mathbf{S} the slope of the isopycnals, defined as $\mathbf{S} = -\nabla_h \rho / \frac{\partial \rho}{\partial z}$. This parameterization conserves the volume of isopycnal layers and thus can maintain fronts much better than pure horizontal diffusion. The term “thickness diffusivity” for κ is not entirely accurate. GM is actually a parameterization for the quasi-Stokes streamfunction (McDougall and McIntosh 2001) and κ should hence be called “quasi-Stokes diffusivity”.

The actual value of κ is not well constrained. GM90 themselves pointed out that κ can vary strongly in space and time. As an example, if κ is diagnosed from eddy-resolving models, it is found that there is considerable vertical structure. In the model used by Eden et al. (2007), κ takes values larger than $1000 \text{ m}^2 \text{ s}^{-1}$ close to the surface of the Southern

Ocean, but it decreases by up to one order of magnitude at depth.

The approach chosen by GWMM95 was to calculate the streamfunction of the eddy-induced velocities from an observational data set (Levitus 1982) using a constant $\kappa = 1000 \text{ m}^2\text{s}^{-1}$. Since this reproduced the meridional heat transports with approximately correct magnitude and meridional distribution, they suggested using a value for κ of this order.

Seeking to improve on using a constant κ , Visbeck et al. (1997) (hereafter cited as Vis97) suggested diagnosing it from the stratification, i.e. the local horizontal and vertical density gradients. Vis97 studied several idealized cases and found that κ varies between $300 \text{ m}^2\text{s}^{-1}$ and $2000 \text{ m}^2\text{s}^{-1}$. Since the vertical density gradient is close to zero in the mixed layer, parameterizations of the Vis97 type can give unrealistically large values for κ . Therefore, tapering schemes must be applied at the boundaries to ensure that the eddy-induced velocity field is non-divergent everywhere (Treguier et al. 1997; Large et al. 1997).

When discussing quasi-Stokes diffusion it is important to point out that, away from the boundaries, the mixing of ocean tracers occurs mainly along isopycnal surfaces (Redi 1982; Griffies et al. 1998; McDougall and Jackett 2005, and many others). This process can be parameterized as downgradient diffusion along the isopycnals, with an isopycnal mixing coefficient κ_{iso} .

Griffies (1998) (hereafter cited as Grif98) formulated the eddy-induced transports in a more elegant and computationally more efficient way than GM90 by writing them as a skew diffusion, instead of a velocity as in (1). The quasi-Stokes diffusivity κ is then incorporated into the mixing tensor and appears in the same terms as κ_{iso} . To simplify the mixing tensor, it is often chosen to have $\kappa_{iso} = \kappa$. A downside of this approach is that the eddy-induced transports are not calculated explicitly anymore, meaning that they are often not available

as a model output.

More recent suggestions to improve the GM parameterization, for instance by diagnosing κ as a three-dimensional field (Hofmann and Maqueda 2011), show an improved response, i.e. closer to what is seen in eddy-resolving models, of the circulation in the Southern Ocean on changes in the surface forcing. However, these approaches are not discussed further here since they have not been used in the AR4 models.

b. Implementations

For the present intercomparison study we gathered information about the individual implementations of the GM parameterization from the documentation available at PCMDI, from the published literature and from personal communication with the modelers. Table 1 shows the results of this effort and goes beyond Russell et al. (2006) and Sen Gupta et al. (2009) in providing these details. Of the 24 models that were studied, three models do not use the GM parameterization (index N), thirteen models use an implementation of GM with a fixed κ (index F), and eight models diagnose κ from the stratification (index V). That is, in the V models κ is a two-dimensional field in latitude and longitude calculated at every time step. The methods vary, but usually involve a vertical integral over the stratification. V refers to Vis97 as one of the first papers introducing this method of calculating κ .

In some models κ is a function of the latitude or mesh size (see footnotes in Table 1), and we used the value at the latitudes of the ACC in these cases. We have classified them as F since κ is then still a constant at any given grid point. Whether the skew flux formulation of Grif98 was employed was not taken into the account for our GM index since, in the light

of the above discussion, this does not affect the strength of the parameterized eddy-induced transports.

For the type F models, the value of κ ranges from $100 \text{ m}^2\text{s}^{-1}$ to $2000 \text{ m}^2\text{s}^{-1}$ (see also Fig. 1a). Some of the type F models are actually isopycnal models, meaning that they use density as a vertical coordinate. These models typically employ interface smoothing. This is physically equivalent to applying GM90 in a depth level model and was therefore subsumed in the same model type. The inter-model spread of κ in the type F models is by and large the same spread that is possible within an individual model of type V , with the exception of the later versions of the OPA ocean model where κ can be as low as $15 \text{ m}^2\text{s}^{-1}$.

3. The Antarctic Circumpolar Current in the AR4 models and in FAMOUS

a. Model data

The ACC is balanced geostrophically by a meridional density gradient that extends from the surface down to below the thermocline. It is still not fully understood how the ACC is driven, however the existing theoretical work (Rintoul et al. 2001; Marshall and Radko 2003) suggests that this meridional density gradient is maintained by fluxes of heat and freshwater at the surface as well as by wind-driven upwelling of dense waters south of the ACC and wind-driven downwelling, or Ekman pumping, north of the ACC. While this wind-driven meridional overturning acts to increase the meridional density gradient, or to steepen the isopycnals, there are substantial eddy-induced transports that flatten the isopycnals. This

mesoscale eddy activity arises from baroclinic instability.

The main quantities used by Russell et al. (2006) in their analysis of the AR4 climate models are the ACC transport, the maximum zonal wind stress and the meridional density difference across the ACC. The actual parameterized eddy-induced transports are not available at the CMIP3 database and therefore could not be analysed. However, κ gives an indication of the strength of the eddy-induced transports (see eq. 1). Therefore we use κ as well as similar diagnostics as Russell et al. (2006) to analyse the type F models. In addition, κ_{iso} is included in the analysis.

We analysed the last twenty years of the control runs (picntrl, averaged from monthly means) and used run 1 if several control runs were available. For the sake of completeness, we obtained additional model data for some models from other public databases (for the GFDL models and for GISS_EH_2) or from the modelling groups directly (for MPIECHAM5). The control runs were chosen because in almost all of them the ACC is close to a statistical equilibrium, with the length of the control runs typically many centuries. To assess possible drifts we analysed the trends of the ACC transport over the last 100 years and found that only three models (4, 5 and 9) have drifts larger than an absolute value of 1 Sv/decade, while seven models have no significant drift, and the rest has drifts of an absolute value of around 0.5 Sv/decade or less. The drift in model 4 is consistently negative over the full length of the control run (500 yr), and therefore we excluded it from the detailed analysis of the type F models. By contrast, in model 5 the magnitude of the drift is decreasing during the control run (length 380 yr), and therefore we retained this model for the detailed analysis. In Figs. 1b) to d) and Figs. 2a) and c), model 11 was left out due to lack of data for the ACC, and model 10 was left out since it uses GM as well as interface smoothing, such that

κ is not representative for all parameterized eddy-induced transports.

The ACC transport was defined as the difference of the barotropic streamfunction across Drake Passage. For five models the barotropic streamfunction was not available. Instead, we calculated the volume transport through Drake Passage from the zonal velocity integrated along 69°W and over the full depth. Using the zonal velocities for all models, instead of the barotropic streamfunction, leads to some minor differences that do not affect our results. Likewise, considering only the baroclinic transports (in the definition by Marshall and Radko 2003) yields similarly small differences for most models, against which our results are robust.

In addition to the AR4 model data, we use the fast atmosphere-ocean GCM (AOGCM) FAMOUS (version XFXWB; Smith et al. 2008; Smith 2011) to explore the impacts of changing κ on the stratification. It is based on the well-established coupled climate model HadCM3 (Gordon et al. 2000). In FAMOUS the resolution was lowered to 2.5° by 3.75° with 20 levels in the ocean and 5° by 7.5° with 11 levels in the atmosphere, with a few resulting adjustments of the model physics. FAMOUS runs fast, simulating up to 250 years per day on 8 processors of a modern server, and thus gives us the opportunity to conduct millennial-scale runs. This is necessary for the full ocean density field to adjust to parameter changes. Yet with most of the AR4 models such long runs could not be conducted due to constraints in computing resources. FAMOUS is a model of type F and uses $\kappa = 1000 \text{ m}^2\text{s}^{-1}$. The control run is more than 5000 years long, and after year 4000 the centennial trends of globally averaged quantities are very small. In model year 4000, two runs were spawned off with $\kappa = 600 \text{ m}^2\text{s}^{-1}$ and $\kappa = 2000 \text{ m}^2\text{s}^{-1}$, sampling the range of the values found among the AR4 models of type F . These two runs, which we call K600 and K2000, were integrated for 1000 years each. In two further runs of 1000 years length, κ_{iso} was varied along with κ , with the same two

values of $\kappa = \kappa_{iso} = 600 \text{ m}^2\text{s}^{-1}$ and $\kappa = \kappa_{iso} = 2000 \text{ m}^2\text{s}^{-1}$. The quantities shown in the figures below are 20-year averages from year 4980 to 5000 of all FAMOUS runs. In terms of globally volume-averaged potential temperature and salinity, the K600 and K2000 runs show clear trends and are not in equilibrium after 1000 yr. However, the ACC transports show no long-term drift after 200 years (not shown).

b. Results

Fig. 1a groups the models' ACC transports by the type of eddy parameterization. Leaving the models without the GM parameterization aside (type *N*), there is no clear distinction between the type *F* and the type *V* models. The type *V* models have a slight tendency towards a stronger ACC: all but one of the models have an ACC transport of 110 Sv or more. Conversely, the type *F* models have a cluster of somewhat weak ACCs around 100 Sv, with the exception of model 5.

Our main result is that there is a clear and significant correlation ($r = -0.79$) of the ACC transport with κ across the type *F* models (Fig. 1b). We chose logarithmic axes in this Figure to better capture the large range of κ values. On linear scales the correlation is $r = -0.68$ and is significant too. The significance is indicated by the low p-value ($p < 0.05$; however the p-value might be an overly confident estimate because the climate models were treated as independent for the calculation of the p-value. Pennell and Reichler (2011) suggest that the actual number of degrees of freedom is lower than the number of AR4 climate models.)

The slope of the regression line in Fig. 1b, based on the AR4 models, is -0.43 ± -0.29 (95% confidence interval from a Student's t-test). This estimate is in line with Danabasoglu

and McWilliams (1995) who used three different values for κ in an ocean-only model. Their resulting ACC transports aligned roughly along a -1/3 slope (their Fig. 3). In addition, a slope of -0.56 can be diagnosed from two runs in Gent et al. (2001). The current estimate includes this value too.

The three FAMOUS runs (red diamonds) align well with the AR4 models in Fig. 1b , suggesting that the spread of ACC transports across the AR4 models can be explained, to some extent, by the spread of κ . This also means that the sensitivities with regard to κ are similar within one model and across different models.

The correlation of the meridional density difference $\Delta\rho_y$ across the ACC with κ is even larger ($r = -0.86$; Fig. 1c). $\Delta\rho_y$ is defined as the density difference between the averaged latitude bands 65°S to 62°S on the one hand and 45°S to 42°S on the other hand, 0-1500 m depth. (With a linear scale for κ , $r = -0.74$.) The pattern of the AR4 models is very similar to Fig. 1b, which is not surprising since $\Delta\rho_y$ represents the geostrophic balance of the ACC. The FAMOUS runs again align very well with the AR4 models, showing that one individual GCM like FAMOUS can map the across-model sensitivity of the AR4 models.

Given the importance of isopycnal diffusion (cf. sec. 2a), we tested whether the ACC transport correlates with κ_{iso} across the type F models (Fig. 1d). It turns out that six out of the nine type F models have $\kappa_{iso} = 1000 \text{ m}^2\text{s}^{-1}$, precluding a significant correlation. The FAMOUS runs with $\kappa_{iso} = \kappa$ (green diamonds in Fig. 1d) show an ACC sensitivity that is very similar to the K600 and K2000 runs, with a somewhat larger response of the ACC transport. In other words, whether only κ or both κ_{iso} and κ are changed makes no substantial difference. This suggests that κ dominates in setting the ACC transport in FAMOUS.

The correlation between the ACC transport and $\Delta\rho_y$ is strong (Fig. 2a) and is retained when all AR4 models are considered (Fig. 2b). Again, this is to be expected because of the geostrophic balance of the ACC. The three FAMOUS runs align very well with the type *F* models.

The influence of κ on the structure of the density field can be seen in more detail in Fig. 3. It shows $\Delta\rho_y(z)$, the zonally averaged density difference across the ACC as a function of depth. $\Delta\rho_y(z)$ is defined like $\Delta\rho_y$ above, apart from the vertical averaging. The dashed lines in Fig. 3 show a selection of the AR4 models, while observations (WOA05 Locarnini et al. 2006; Antonov et al. 2006) are plotted with a dash-dotted line and the FAMOUS runs are represented by solid lines.

The vertical structure of $\Delta\rho_y(z)$ differs substantially among the models in Fig. 3. For instance, above 2300m depth model 20 has a larger $\Delta\rho_y(z)$ than model 18, while below 2300m depth model 20 has a small $\Delta\rho_y(z)$ that even turns negative below 3500m depth. This explains plausibly why model 18 has the greater ACC transport (Fig. 1b) in spite of the smaller $\Delta\rho_y(z)$ above 2300m depth. The vertical density structure in the latitude band north of the ACC can also have a marked impact on projected changes of the ACC transport (Wang et al. 2011).

The differences of $\Delta\rho_y(z)$ among the FAMOUS runs (solid lines in Fig. 3) are consistent with the differences between the AR4 models. Compared with observations (dash-dotted), the ACC in FAMOUS is too strong in the top 500 m and too weak below that. Still, Fig. 3 shows the top-to-bottom influence of κ on the horizontal density gradient: increasing κ leads to a larger tendency to restratify, reducing $\Delta\rho_y(z)$. Note that the deviation of FAMOUS from observations is not an outlier in comparison with the full set of AR4 models (not shown).

We looked at the density changes in FAMOUS in more detail. Fig. 4 shows the zonally averaged density fields of the control run (Fig. 4a) and the anomalies of both K600 (Fig. 4b) and K2000 (Fig. 4c). Below the surface layer (top 100 m) the changes are as expected. In the K600 run there is a smaller tendency for restratification. Thus the isopycnals have a larger tilt, leading to lighter waters (blue shading) north of the ACC and denser waters (red shading) south of the ACC. In the K2000 run this effect is reversed. In the surface layer however this simple relationship does not hold. While the surface density anomalies are in line with the subsurface anomalies in the K2000 run, there is a positive density anomaly everywhere in the surface layer in the K600 run. This effect is predominantly due to salinity anomalies (not shown) and might come from the surface tapering used in the GM parameterization. These surface effects merit a deeper investigation, which is beyond the scope of this note.

We now discuss the correlation of the ACC transport with the maximum of the zonally averaged wind stress τ^x in the AR4 models as well as in FAMOUS. Fig. 2 shows the correlations for the type F models (panel c) and, for comparison, for all AR4 models (panel d). For the type F models (Fig. 2c), the correlation of the ACC transport with τ^x is somewhat lower than with κ or with $\Delta\rho_y$, and if all AR4 models are considered (Fig. 2d) there is no significant correlation any more. The FAMOUS runs (red diamonds) do not align with the AR4 models because the wind stress changes are very small. These results indicate that the wind stress is not the dominant factor in explaining the spread of the simulated ACC transports. This can also be seen by comparing pairwise some of the AR4 models. For instance, models 3 and 20 have virtually the same maximum zonally averaged zonal wind stress τ^x , but their ACC transports differ by more than 50 Sv (Fig. 2c). This discrepancy is

well explained by the difference in κ , which is $200 \text{ m}^2\text{s}^{-1}$ for model 20 and $1000 \text{ m}^2\text{s}^{-1}$ for model 3 (Fig. 1b). Model 18 and model 2 compare in a very similar way, and the $\Delta\rho_y(z)$ profiles in these four models are consistent with their ACC transports (Fig. 3). Still, for models with the same value of κ (e.g. models 2, 3 and 13 in Fig. 1b), the varying strength of the wind stress can explain the different ACC transports.

We believe that we analysed the most important diagnostics with regard to influence on the ACC transport. There are however more diagnostics that could be studied. For example, we have not investigated the dependence of the ACC transport on horizontal viscosity because its influence on the ACC is unclear so far. Sensitivity studies with fully coupled GCMs can show, for a lower viscosity, a strengthened ACC transport (Griffies et al. (2005), with GFDL CM 2.1) or a weakened ACC transport (Jochum et al. (2008), with NCAR CCSM3). A clarification of the role of viscosity in setting the ACC transport would be a study in its own right and is not pursued here. One other property that is relevant for the ACC dynamics is the bottom topography. It can influence the ACC transport by its role in defining the bottom form stress, which balances the wind stress at the surface. Calculating the bottom form stress from the available AR4 model data turned out to be not feasible because of the loss of accuracy from the spatial interpolation of the data which was applied to many models' output. Using simple measures of the models' bottom topography instead, we could not find a correlation of the ACC with, for instance, the maximum unobstructed depth at Drake Passage latitudes or with the width of Drake Passage in grid points across the models.

4. Discussion

In this note we have investigated the role of parameterized eddy-induced transports in determining the transport of the ACC across the control runs of the AR4 models and in a coarse-resolution GCM. Due to the lack of data on eddy-induced transports from the AR4 models, we used the main parameter of the GM parameterization for this purpose. For those models where this quasi-Stokes diffusivity κ is not diagnosed from the density field and therefore not time-dependent (type F), κ is a powerful parameter. The ACC transport and the meridional density difference $\Delta\rho_y$ correlate significantly with κ . Experiments with the fast AOGCM FAMOUS reproduce the across-model relationship between the ACC transport, κ and the meridional density gradient. In other words, the dependence of the ACC as well as the meridional density gradient on κ is very similar across the type F subset of the AR4 ensemble, containing nine different models, and among several runs of an individual model (FAMOUS).

For the isopycnal diffusivity κ_{iso} an across-model correlation with the ACC transport could not be found. Additional FAMOUS experiments show that the ACC transport is more sensitive to κ than to κ_{iso} .

The correlation of the ACC with the maximum of the zonally averaged zonal wind stress is weaker than with κ . Variations in κ can explain the varying ACC transport between type F models with the same wind stress maximum. The FAMOUS experiments show as well that different equilibrium ACC transports can exist under very similar maximum zonal wind stresses. All this indicates that the density structure in the ocean is dominant over the maximum of the zonal wind stress in setting the ACC transport. The use of a fully

coupled climate model for this purpose is an advantage over earlier GM sensitivity studies (Danabasoglu and McWilliams 1995; Gent et al. 2001) that used an ocean-only setup.

It would have been very interesting to include the type V models by diagnosing the κ values from their density fields. This is however cumbersome as the exact details of the implementation of the GM parameterization would have to be known, given that for the AR4 models the actual eddy-induced transports are not available. Also, previous studies show that there is no consensus at all about the projected 21st century changes of the ACC, not even about the sign (Sen Gupta et al. 2009; Wang et al. 2011). The role of the parameterized eddy-induced transports in these diverse responses needs to be understood. For these reasons, it would be of great value within the ongoing CMIP5 intercomparison if modelling groups would diagnose these transports and make the data available.

The latest generation of GCMs, which is currently being used to produce simulations for the upcoming Fifth Assessment Report of the IPCC, begins to have eddy-permitting oceans with resolutions of $1/3^\circ$ or higher, where the GM parameterization is not employed any more (Shaffrey et al. 2009; Delworth et al. 2012). If eddies are resolved (or permitted) the response of the ACC to changes in wind stress becomes clearly smaller (Hallberg and Gnanadesikan 2006; Farneti et al. 2010). However, the computational cost of eddy-permitting ocean components is still far too high if they carry many tracers, for instance as part of a carbon cycle model. Therefore in the nearer future the GM parameterization will still be in use, and the present note demonstrates that κ is likely to be the strongest determinant of the transport of the ACC in models. We therefore recommend testing the sensitivity of the circulation against varying κ .

Acknowledgments

We acknowledge the modeling groups for making their model output available for analysis, the PCMDI for collecting and archiving this data, and the WCRP’s Working Group on Coupled Modelling (WGCM) for organizing the model data analysis activity. We are grateful to Johann Jungclaus for giving us access to the control run of MPI_ECHAM5. The research leading to these results has received funding from the European Research Council under the European Community’s Seventh Framework Programme (FP7/2007-2013), ERC grant agreement number 247220, project “Seachange”. In addition, TK was supported by a Marie Curie Intra-European Fellowship within the 7th European Community Framework Programme. FAMOUS was integrated on HECToR, the UK National Supercomputing resource.

REFERENCES

- 379 Antonov, J. I., Locarnini, R. A., Boyer, T. P., Mishonov, A. V., , Garcia, H. E., 2006. World
380 Ocean Atlas 2005. Vol. 2 of NOAA Atlas NESDIS 62. U.S. Government Printing Office,
381 Washington, D.C., US, p. 182.
- 382 Bleck, R., 2002. An oceanic general circulation model framed in hybrid isopycnic-Cartesian
383 coordinates. *Ocean Modelling* 37, 55–88.
- 384 Cunningham, S. A., Alderson, S. G., King, B. A., Brandon, M. A., 2003. Transport and vari-
385 ability of the Antarctic Circumpolar Current in Drake Passage. *J. Geophys. Res.* 108 (C5),
386 8084.
- 387 Danabasoglu, G., Large, W. G., Tribbia, J. J., Gent, P. R., Briegleb, B. P., 2006. Diurnal
388 coupling in the tropical oceans of CCSM3. *J. Clim.* 19, 2347–2365.
- 389 Danabasoglu, G., McWilliams, J., 1995. Sensitivity of the global ocean circulation to param-
390 eterizations of mesoscale tracer transports. *J. Clim.* 8, 2967–2987.
- 391 Delworth, T. L., Rosati, A., Anderson, W., Adcroft, A. J., Balaji, V., Benson, R., Dixon,
392 K., Griffies, S. M., Lee, H.-C., Pacanowski, R. C., Vecchi, G. A., Wittenberg, A. T.,
393 Zeng, F., Zhang, R., 2012. Simulated climate and climate change in the GFDL CM2.5
394 high-resolution coupled climate model. *J. Clim.* 25 (8), 2755–2781.
- 395 Diansky, N. A., Bagno, A. V., Zalesny, V. B., 2002. Sigma model of global ocean circulation

and its sensitivity to variations in wind stress. *Izvestiya, Atmospheric and Oceanic Physics*
38 (4), 477–494.

Eden, C., Greatbatch, R. J., Willebrand, J., 2007. Diagnosis of thickness fluxes in an eddy-resolving model. *J. Phys. Oceanogr.* 37, 727–742.

Farneti, R., Delworth, T. L., Rosati, A. J., Griffies, S. M., Zeng, F., 2010. The role of mesoscale eddies in the rectification of the Southern Ocean response to climate change. *J. Phys. Oceanogr.* 40, 1539–1557.

Farneti, R., Gent, P. R., 2011. The effects of the eddy-induced advection coefficient in a coarse-resolution coupled climate mode. *Ocean Modelling* 39 (1-2), 135–145.

Furevik, T., Bentsen, M., Drange, H., Kindem, I. K. T., Kvamstø, N. G., Sorteberg, A., 2003. Description and validation of the Bergen Climate Model: ARPEGE coupled with MICOM. *Clim. Dyn.* 21, 27–51.

Gent, P. R., Large, W. G., Bryan, F. O., 2001. What sets the mean transport through Drake Passage? *J. Geophys. Res.* 106 (C2), 2693–2712.

Gent, P. R., McWilliams, J. C., 1990. Isopycnal mixing in ocean circulation models. *J. Phys. Oceanogr.* 20, 150–155.

Gent, P. R., Willebrand, J., McDougall, T. J., McWilliams, J. C., 1995. Parameterizing eddy-induced tracer transports in ocean circulation models. *J. Phys. Oceanogr.* 25, 463–474.

Gordon, C., Cooper, C., Senior, C., Banks, H., Gregory, J., Johns, T., Mitchell, J., Wood,

R., 2000. The simulation of SST, sea ice extents and ocean heat transports in a version of the Hadley Centre coupled model without flux adjustments. *Clim. Dyn.* 16, 147–168.

Gordon, H., O’Farrell, S., Collier, M., Dix, M., Rotstayn, L., Kowalczyk, E., Hirst, T., Watterson, I., 2010. The CSIRO Mk3.5 climate system model. CAWCR Technical Report No.021.

Gordon, H., Rotstayn, L., McGregor, J., Dix, M., Kowalczyk, E., O’Farrell, S., Waterman, L., Hirst, A., Wilson, S., Collier, M., Watterson, I., Elliott, T., 2002. The CSIRO Mk3 climate system model. CSIRO Atmospheric Research Technical Paper No.60.

Griffies, S. M., 1998. The Gent–McWilliams skew flux. *J. Phys. Oceanogr.* 28, 831–841.

Griffies, S. M., Böning, C., Bryan, F. O., Chassignet, E. P., Hasumi, H., Hirst, A., Treguier, A.-M., Webb, D., 2000. Developments in ocean climate modelling. *Ocean Modelling* 2, 123–192.

Griffies, S. M., Gnanadesikan, A., Dixon, K., Dunne, J. P., Gerdes, R., Harrison, M. J., Rosati, A., Russell, J. L., Samuels, B. L., Spelman, M. J., M.Winton, Zhang, R., 2005. Formulation of an ocean model for global climate simulations. *Ocean Science* 1, 45–79.

Griffies, S. M., Gnanadesikan, A., Pacanowski, R. C., Larichev, V. D., Dukowicz, J. K., Smith, R. D., 1998. Isonutral diffusion in a z-coordinate ocean model. *J. Phys. Oceanogr.* 28, 805–830.

Hallberg, R., Gnanadesikan, A., 2006. The role of eddies in determining the structure and response of the wind-driven Southern Hemisphere overturning: Results from the modeling eddies in the Southern Ocean project. *J. Phys. Oceanogr.* 36, 2232–2252.

437 Hasumi, H., Emori, S., K-1 model developers, September 2004. K-1 Coupled GCM (MIROC)
 438 description. K-1 Technical Report No. 1.

439 Hofmann, M., Maqueda, M. A. M., 2011. The response of Southern Ocean eddies to increased
 440 midlatitude westerlies: A non-eddy resolving model study. *Geophys. Res. Lett.* 38, L03605,
 441 doi:10.1029/2010GL045972.

442 IPCC, 2007. *Climate Change 2007: The Physical Science Basis. Contribution of Working*
 443 *Group I to the Fourth Assessment Report of the Intergovernmental Panel on Climate*
 444 *Change.* S. Solomon and D. Qin and M. Manning and Z. Chen and M. Marquis and K.B.
 445 Averyt and M. Tignor and H.L. Miller (eds.): Cambridge University Press, Cambridge,
 446 UK, and New York, NY, USA, 996 pp.

447 Jochum, M., Danabasoglu, G., Holland, M., Kwon, Y.-O., Large, W. G., 2008. Ocean vis-
 448 cosity and climate. *J. Geophys. Res.* 113, C06017.

449 Kim, S.-J., Flato, G., Boer, G., McFarlane, N., 2002. A coupled climate model simulation
 450 of the Last Glacial Maximum, Part 1: transient multi-decadal response. *Clim. Dyn.* 19,
 451 515–537.

452 Large, W. G., Danabasoglu, G., Doney, S. C., McWilliams, J. C., 1997. Sensitivity to surface
 453 forcing and boundary layer mixing in a global ocean model: Annual-mean climatology. *J.*
 454 *Phys. Oceanogr.* 27 (11), 2418–2447.

455 Levitus, S., 1982. *Climatological atlas of the world ocean.* Tech. Rep. NTIS PB83-184093,
 456 NOAA/ERL GFDL, Princeton, N.J.

457 Locarnini, R. A., Mishonov, A. V., Antonov, J. I., Boyer, T. P., Garcia, H. E., 2006. World
 458 Ocean Atlas 2005. Vol. 1 of NOAA Atlas NESDIS 61. U.S. Government Printing Office,
 459 Washington, D.C., US, p. 182.

460 Madec, G., Delecluse, P., Imbard, M., Lévy, C., Dec. 1998. OPA 8.1 Ocean General Circu-
 461 lation Model reference manual. Notes du Pôle de Modélisation, No. 11.

462 Marshall, J., Radko, T., 2003. Residual-mean solution for the Antarctic Circumpolar Current
 463 and its associated overturning circulation. *J. Phys. Oceanogr.* 33, 2341–2354.

464 Marsland, S., Haak, H., Jungclaus, J., Latif, M., Röske, F., 2003. The Max-Planck-Institute
 465 global ocean/sea ice model with orthogonal curvilinear coordinates. *Ocean Modelling* 5,
 466 91–127.

467 McDougall, T. J., Jackett, D. R., 2005. The material derivative of neutral density. *J. Mar.*
 468 *Res.* 63, 159–185.

469 McDougall, T. J., McIntosh, P., 2001. The temporal-residual-mean velocity. Part II: isopy-
 470 cnal interpretation and the tracer and momentum equations. *J. Phys. Oceanogr.*, 1222–
 471 1246.

472 Pennell, C., Reichler, T., 2011. On the effective number of climate models. *J. Clim.* 24,
 473 2358–2367.

474 Redi, M., 1982. Oceanic isopycnal mixing by coordinate rotation. *J. Phys. Oceanogr.* 12,
 475 1154–1158.

476 Rintoul, S. R., Hughes, C. W., Olbers, D., 2001. The Antarctic Circumpolar Current system.
 477 In: Siedler, G. (Ed.), *Ocean Circulation and Climate*. Academic Press, pp. 271–301.

478 Risien, C. M., Chelton, D. B., 2008. A global climatology of surface wind and wind stress
 479 fields from eight years of QuikSCAT scatterometer data. *J. Phys. Oceanogr.* 38, 2379–2413.

480 Roberts, M. J., 2004. The Gent and McWilliams parameterisation scheme, including Visbeck
 481 and biharmonic GM schemes. *Unified Model Documentation Paper UMDP54*, 23 pp.

482 Russell, G. L., Miller, J. R., Rind, D., 1995. A coupled atmosphere-ocean model for transient
 483 climate change studies. *Atmosphere-Ocean* 33 (4), 683–730.

484 Russell, J. L., Stouffer, R. J., Dixon, K., 2006. Intercomparison of the Southern Ocean
 485 circulations in IPCC model control simulations. *J. Clim.* 19, 4560–4575.

486 Saenko, O. A., Fyfe, J. C., England, M. H., 2005. On the response of the oceanic wind-driven
 487 circulation to atmospheric CO₂ increase. *Clim. Dyn.* 25 (4), 415–426.

488 Sen Gupta, A., Santoso, A., Taschetto, A. S., Ummenhofer, C. C., Trevena, J., England,
 489 M. H., 2009. Projected changes to the southern hemisphere ocean and sea ice in the IPCC
 490 AR4 climate models. *J. Clim.* 22, 3047–3078.

491 Shaffrey, L. C., Stevens, I., Norton, W. A., Roberts, M. J., Vidale, P. L., Harle, J. D.,
 492 Jrrar, A., Stevens, D. P., Woodage, M. J., Demory, M. E., Donners, J., Clark, D. B.,
 493 Clayton, A., Cole, J. W., Wilson, S. S., Connolley, W. M., Davies, T. M., Iwi, A. M.,
 494 Johns, T. C., King, J. C., New, A. L., Slingo, J. M., Slingo, A., Steenman-Clark, L.,
 495 Martin, G. M., 2009. U.K. HiGEM: The new U.K. high-resolution global environment
 496 model—Model description and basic evaluation. *J. Clim.* 22, 1861–1896.

- Sijp, W. P., Bates, M., England, M., 2006. Can isopycnal mixing control the stability of the thermohaline circulation in ocean climate models? *J. Clim.* 19 (21), 5637–5651.
- Smith, R. S., 2011. The FAMOUS climate model (versions XFXWB and XFHCC): description update to version XDBUA. *Geoscientific Model Development Discussions* 4, 3047–3065.
- Smith, R. S., Gregory, J. M., Osprey, A., 2008. A description of the FAMOUS (version XDBUA) climate model and control run. *Geoscientific Model Development* 1 (1), 53–68.
- Sun, S., Bleck, R., 2006. Multi-century simulations with the coupled GISS–HYCOM climate model: control experiments. *Clim. Dyn.* 26, 407–428.
- Treguier, A., Held, I., Larichev, V., 1997. Parameterization of quasigeostrophic eddies in primitive equation ocean models. *J. Phys. Oceanogr.* 27, 567–580.
- Visbeck, M., Marshall, J., Haine, T., Spall, M., 1997. Specification of eddy transfer coefficients in coarse-resolution ocean circulation models. *J. Phys. Oceanogr.* 27, 381–402.
- Wang, Z., Kuhlbrodt, T., Meredith, M. P., 2011. On the response of the Antarctic Circumpolar Current transport to climate change in coupled climate models. *J. Geophys. Res.* 116, C08011.
- Woloszyn, M., Mazloff, M., Ito, T., 2011. Testing an eddy-permitting model of the Southern Ocean carbon cycle against observations. *Ocean Modelling* 39 (1-2), 170–182.
- Wright, D. K., 1997. A new eddy mixing parametrization and ocean general circulation model. *International WOCE Newsletter* 26, 27–29.

517 Yukimoto, S., Noda, A., Kitoh, A., Sugi, M., Kitamura, Y., Hosaka, M., Shibata, K., Maeda,
518 S., Uchiyama, T., Feb 2001. The new Meteorological Research Institute Coupled GCM
519 (MRI-CGCM2) – Model climate and variability. Papers in Meteorology and Geophysics
520 51 (2), 47–88.

TABLE 1. Parameterizations of eddy-induced transports in the IPCC AR4 global coupled climate models. The GM index i_{GM} is either N if such a parameterization is absent, F for a fixed quasi-Stokes diffusivity κ or V if κ varies as a function of the density field at each time step. “IS” stands for the interface smoothing that is used in isopycnal models. It is equivalent to applying GM. Of the references the first one (before the slash) gives the actual value of κ , if applicable. “PCMDI” refers to the online documentation available at http://www-pcmdi.llnl.gov/ipcc/model_documentation/ipcc_model_documentation.php.

No.	GCM name	Ocean model	Eddy parameterization	i_{GM}	κ [m ² s ⁻¹]	References for GM implementation
1	BCCR_BCM2_0	MICOM 2.8	IS (isopycnal model)	F	–	–/ Furevik et al. (2003)
2	CCCMA_CGCM3_1_T47	MOM1.1	GM90	F	1000	Saenko et al. (2005)/ Kim et al. (2002)
3	CCCMA_CGCM3_1_T63	MOM1.1	GM90	F	1000	Saenko et al. (2005)/ Kim et al. (2002)
4	CNRM_CM3	OPA8.1	GM90	F	2000	PCMDI/ Madec et al. (1998)
5	CSIRO_MK3_0	MOM2.2	GM90, Grif98	F	100	Gordon et al. (2002)
6	CSIRO_MK3_5	MOM2.2	Vis97, Grif98	V	100 to 600 ^a	Gordon et al. (2010)
7	GFDL_CM2_0	OM3.0	Griffies et al. (2005), Grif98	V	100 to 600 ^a	Griffies et al. (2005)
8	GFDL_CM2_1	OM3.1	Griffies et al. (2005), Grif98	V	100 to 600 ^a	Griffies et al. (2005)
9	GISS_AOM	Russell	none	N	–	–/ Russell et al. (1995)
10	GISS_EH_2	HYCOM	GM90 and IS (isopycnal model)	F	1000 to 4000 ^b	Sun and Bleck (2006)
11	GISS_EH	HYCOM	IS (isopycnal model)	F	100 ^c	PCMDI/ Bleck (2002)
12	GISS_ER	Russell	Vis97, Grif98	V	–	–/ Russell et al. (1995), PCMDI
13	IAP_FGOALS1_0_G	LICOM1.0	GM90	F	1000	Hailong Liu, pers. comm./ PCMDI
14	INGV_ECHAM4	OPA8.2	Treguier et al. (1997)	V	15 to 2000 ^a	PCMDI/ Madec et al. (1998)
15	INMCM3_0	^d	none (σ levels)	N	–	–/ Diansky et al. (2002)
16	IPSL_CM4	OPA8.1	Treguier et al. (1997)	V	15 to 2000 ^a	PCMDI/ Madec et al. (1998)
17	MIROC3_2_HIRES	COCO3.0	GWMM95	F	700 ^e	Hasumi et al. (2004)
18	MIROC3_2_MEDRES	COCO3.0	GWMM95	F	700	Hasumi et al. (2004)
19	MIUB_ECHO_G	HOPE-G	none	N	–	–
20	MPI_ECHAM5	MPI-OM	GWMM95, Grif98	F	200 ^f	Johann Jungclaus, pers. comm./ Marsland et al. (2003)
21	MRI_CGCM2_3_2	^d	GM90	F	2000	Yukimoto et al. (2001)
22	NCAR_CCSM3_0	POP	GM90, Grif98	F	600	Danabasoglu et al. (2006)
23	NCAR_PCM1 ^g	–	–	–	–	–
24	UKMO_HADCM3	^d	GWMM95, Vis97, Wright (1997)	V	300 to 2000 ^a	Wright (1997)
25	UKMO_HADGEM1	^d	Vis97, Grif98, Roberts (2004)	V	150 to 2000 ^a	Roberts (2004)

^amin. to max. range imposed on variable κ formulation

^bdepends on mesh size as a function of latitude only

^cestimated equivalent value

^dno well-known name as a stand-alone model

^evalue south of 50° lat.; $\kappa=0$ north of 40° lat., with a linear increase in between

^fvalue in latitudes of the ACC; actual value depends on mesh size in rotated grid

^gdisregarded for this study since no control run available

List of Figures

- 1 (a) The AR4 climate models (blue squares; numbers see Table 1) sorted by the ACC transport (volume transport through Drake Passage) and the GM index (see text for definition). Red diamond: FAMOUS control run. (b) The ACC transport against the value of the quasi-Stokes diffusivity κ on logarithmic scales. Blue squares show the AR4 models, but only the type *F* models, where κ is constant or at most a function of latitude, are included. Red diamonds show the FAMOUS model runs. (c) The zonally averaged meridional density gradient across the ACC against κ , for the type *F* AR4 models (blue squares) and those FAMOUS runs where κ was varied (red diamonds). The scale for κ is logarithmic. (d) The ACC transport against κ_{iso} , for the type *F* models (blue squares) and those FAMOUS runs where κ and κ_{iso} were varied (green diamonds). The scale for κ_{iso} is logarithmic. Here and in Fig. 2, the black lines are the regression lines, and the correlation and regression coefficients are calculated from the AR4 models, excluding FAMOUS. In panel d) the first regression coefficient is not significant.

31

- 2 Upper row: the ACC transport against the meridional density difference
 $\Delta\rho_y$ across the ACC for (a) the type F models and (b) all AR4 models.
Lower row: the ACC transport against the maximum zonally averaged wind
stress τ^x over the Southern Ocean for (c) the type F models and (d) all AR4
models. In all panels, the red diamonds represent the FAMOUS model runs
(where only κ was varied). There is no significant correlation with τ^x if all
AR4 models are considered, while a correlation with $\Delta\rho_y$ is retained. In (d)
the crosses denotes the mean value from the last 100 years of the control
runs, and the error bars show one standard deviation (of the annual means).
Since the standard deviations are very small for most models, simple squares
represent the models in the other panels as well as in Fig. 1. In all panels the
black asterisk indicates observational values. These are from Cunningham et
al., 2003, for the ACC; Risien and Chelton, 2008, for the wind stress (from
QuikSCAT); and the World Ocean Atlas 2005 (Locarnini et al., 2006; Antonov
et al., 2006) for the density difference. 32
- 3 Zonally averaged density difference $\Delta\rho_y(z)$ across the ACC, as a function of
depth, for the FAMOUS runs (solid lines), four of the AR4 models (dashed
lines) and from observations (World Ocean Atlas 2005; dash-dotted). The
dotted vertical line marks $\Delta\rho_y(z) = 0$. $\Delta\rho_y(z)$ is defined as the potential
density (σ_0) difference between the averaged latitude bands 65°S to 62°S on
the one hand and 45°S to 42°S on the other hand. 33

4 Potential density σ_0 of the FAMOUS model runs in the Southern Ocean,
averaged zonally and over the last 20 years of the runs. (a) Control run; (b)
anomalies of K600; (c) anomalies of K2000. Below 100m depth, the patterns
in (b) and (c) are very similar, but with the opposite sign, reflecting the effect
on the stratification of decreasing/ increasing κ . 34

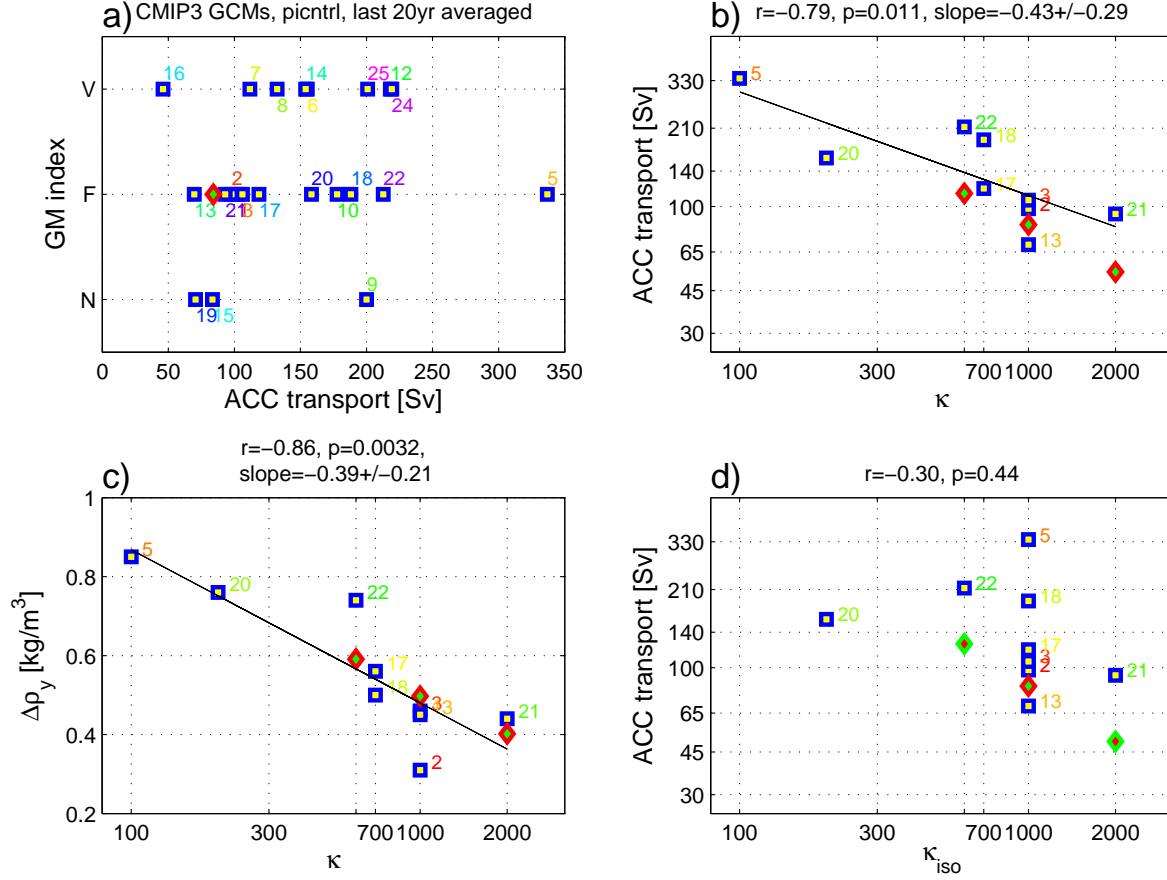


FIG. 1. (a) The AR4 climate models (blue squares; numbers see Table 1) sorted by the ACC transport (volume transport through Drake Passage) and the GM index (see text for definition). Red diamond: FAMOUS control run. (b) The ACC transport against the value of the quasi-Stokes diffusivity κ on logarithmic scales. Blue squares show the AR4 models, but only the type *F* models, where κ is constant or at most a function of latitude, are included. Red diamonds show the FAMOUS model runs. (c) The zonally averaged meridional density gradient across the ACC against κ , for the type *F* AR4 models (blue squares) and those FAMOUS runs where κ was varied (red diamonds). The scale for κ is logarithmic. (d) The ACC transport against κ_{iso} , for the type *F* models (blue squares) and those FAMOUS runs where κ and κ_{iso} were varied (green diamonds). The scale for κ_{iso} is logarithmic. Here and in Fig. 2, the black lines are the regression lines, and the correlation and regression coefficients are calculated from the AR4 models, excluding FAMOUS. In panel d) the first regression coefficient is not significant.

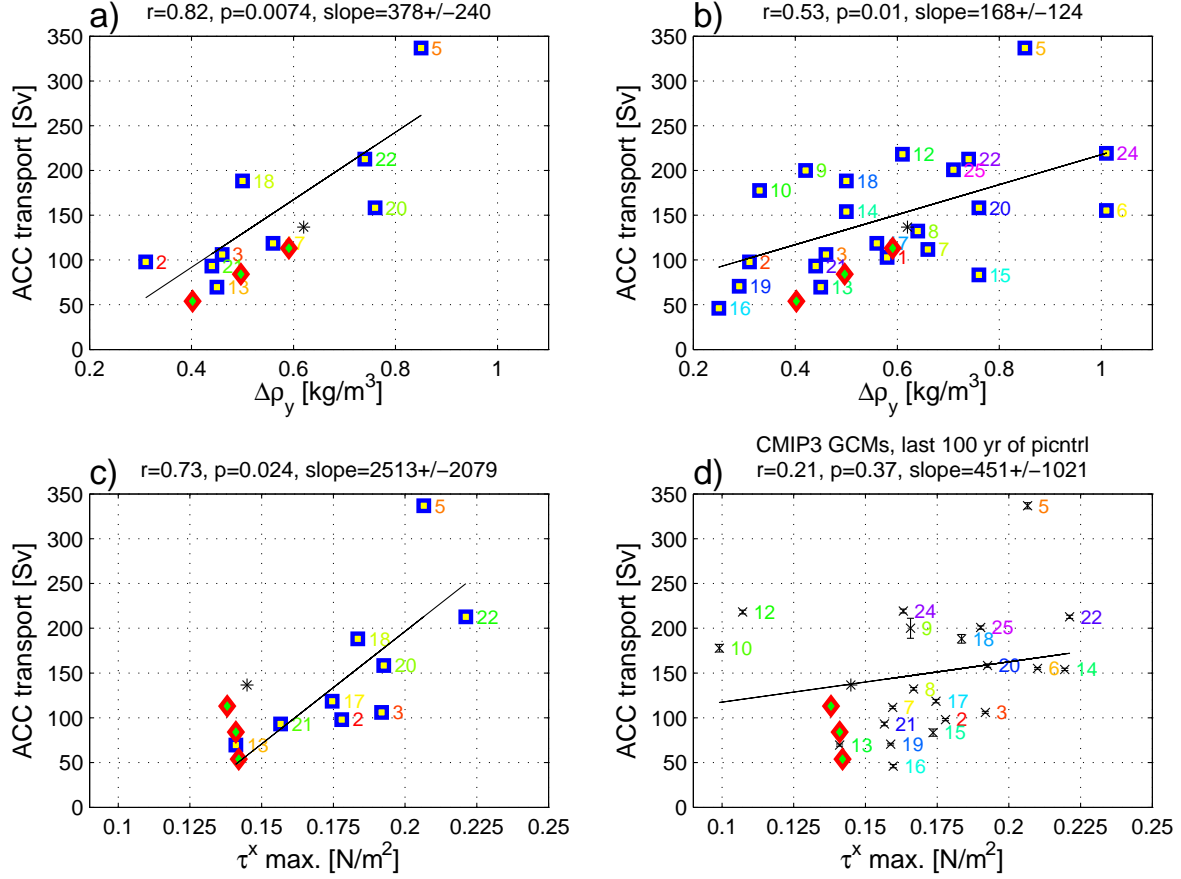


FIG. 2. Upper row: the ACC transport against the meridional density difference $\Delta\rho_y$ across the ACC for (a) the type *F* models and (b) all AR4 models. Lower row: the ACC transport against the maximum zonally averaged wind stress τ^x over the Southern Ocean for (c) the type *F* models and (d) all AR4 models. In all panels, the red diamonds represent the FAMOUS model runs (where only κ was varied). There is no significant correlation with τ^x if all AR4 models are considered, while a correlation with $\Delta\rho_y$ is retained. In (d) the crosses denotes the mean value from the last 100 years of the control runs, and the error bars show one standard deviation (of the annual means). Since the standard deviations are very small for most models, simple squares represent the models in the other panels as well as in Fig. 1. In all panels the black asterisk indicates observational values. These are from Cunningham et al., 2003, for the ACC; Risien and Chelton, 2008, for the wind stress (from QuikSCAT); and the World Ocean Atlas 2005 (Locarnini et al., 2006; Antonov et al., 2006) for the density difference.

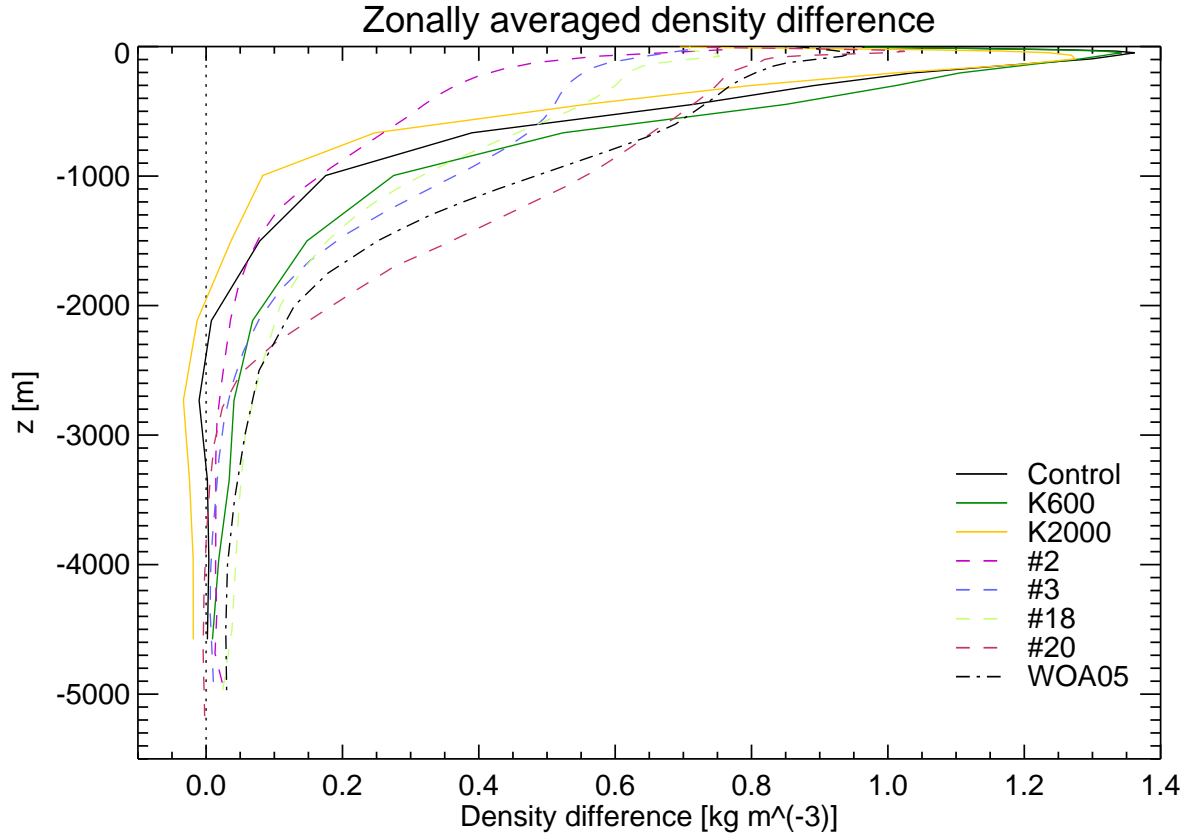


FIG. 3. Zonally averaged density difference $\Delta\rho_y(z)$ across the ACC, as a function of depth, for the FAMOUS runs (solid lines), four of the AR4 models (dashed lines) and from observations (World Ocean Atlas 2005; dash-dotted). The dotted vertical line marks $\Delta\rho_y(z) = 0$. $\Delta\rho_y(z)$ is defined as the potential density (σ_0) difference between the averaged latitude bands 65°S to 62°S on the one hand and 45°S to 42°S on the other hand.

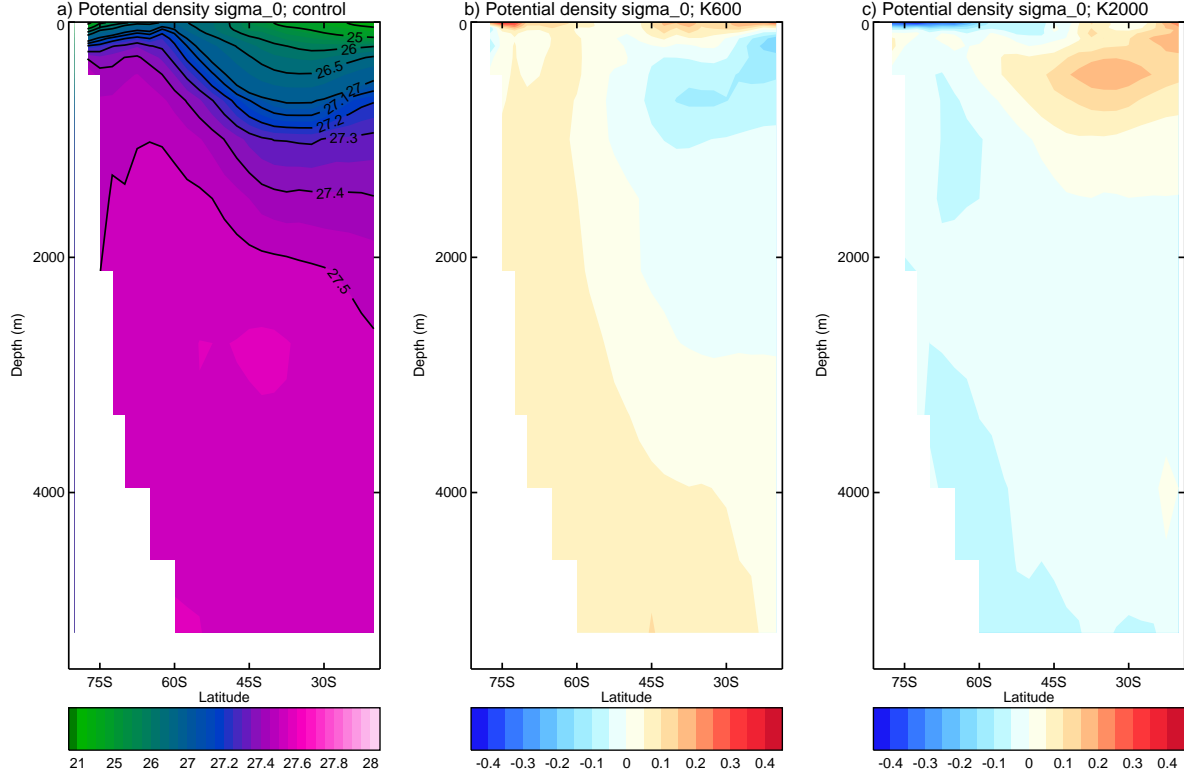


FIG. 4. Potential density σ_0 of the FAMOUS model runs in the Southern Ocean, averaged zonally and over the last 20 years of the runs. (a) Control run; (b) anomalies of K600; (c) anomalies of K2000. Below 100m depth, the patterns in (b) and (c) are very similar, but with the opposite sign, reflecting the effect on the stratification of decreasing/ increasing κ .